Front. Earth Sci. 2021, 15(4): 770–789
https://doi.org/10.1007/s11707-021-0888-7

RESEARCH ARTICLE

Mechanism of pore pressure variation in multiple coal reservoirs, western Guizhou region, South China

Wei JU (✉)[1,2], Zhaobiao YANG[1,2], Yulin SHEN[1,2], Hui YANG[2], Geoff WANG[3], Xiaoli ZHANG[2], Shengyu WANG[2]

1 Key Laboratory of Coalbed Methane Resources and Reservoir Formation Process (Ministry of Education), China University of Mining and Technology, Xuzhou 221008, China
2 School of Resources and Geosciences, China University of Mining and Technology, Xuzhou 221116, China
3 School of Chemical Engineering, The University of Queensland, Brisbane St Lucia 4072, Australia

Abstract Pore pressure is an important parameter in coalbed methane (CBM) exploration and development; however, the distribution pattern and mechanism for pore pressure differences in the Upper Permian CBM reservoirs are poorly understood in the western Guizhou region of South China. In this study, lateral and vertical variations and mechanisms for pore pressure differences are analyzed based on 126 injection-falloff and *in-situ* stress well test data measured in Permian coal reservoirs. Generally, based on the pore pressure gradient and coefficient in coal reservoirs of the western Guizhou region, five zones can be delineated laterally: the mining areas of Zhina, northern Liupanshui, northern Guizhou, northwestern Guizhou and southern Liupanshui. Vertically, there are two main typical patterns: i) the pore pressure gradient (or coefficient) is nearly unchanged in different coal reservoirs, and ii) the pore pressure gradient (or coefficient) has cyclic variations in a borehole profile with multiple coal seams, which suggests the existence of a "superimposed CBM system". The mechanism analysis indicates that coal permeability, thermal evolution stage and hydrocarbon generation contribute little to pore pressure differences in coal reservoirs in the western Guizhou region. The present-day *in-situ* stress field, basement structure and tectonic activity may be the dominant factors affecting lateral pore pressure differences. The sealing capacity of caprocks and the present-day *in-situ* stress field are significant parameters causing vertical pore pressure differences in coal reservoirs. These results are expected to provide new geological references for CBM exploration and development in the western Guizhou region.

Received September 17, 2020; accepted January 20, 2021

E-mail: wju@cumt.edu.cn

Keywords pore pressure difference, influencing factor, coalbed methane reservoir, Upper Permian, western Guizhou region

1 Introduction

Pore pressure (or formation pressure) is commonly defined as the pressure on the fluids inside pore spaces of a porous formation, and is one of the most important parameters for geomechanical and geological analysis (Veeken, 2007; Xu et al., 2011; Zhang, 2011; Khoshnaw et al., 2014). Generally, in normal situations, pore fluids are assumed to be in hydrostatic equilibrium all the way from the surface to the attained depth; however, pore pressures in some subsurface sedimentary formations are not hydrostatic due to the various geological processes (Zahid and Uddin, 2005; Tingay et al., 2009; Dasgupta et al., 2016; Ju et al., 2018a; Saxena et al., 2018). If pore pressure is less than or exceeds hydrostatic pressure, which is defined as the pressure exerted by a continuous column of static fluid (Osborne and Swarbrick, 1997), it produces abnormal pore pressure. In this study, based on the pressure gradient and/or pressure coefficient, pore pressure is classified into three types, namely, underpressure, normal pressure and overpressure (Table 1). There are many causes of overpressure including disequilibrium compaction, tectonic compression, aquathermal expansion, mineral dehydration, hydrocarbon generation, vertical fluid movement, mineral transformation and hydrocarbon buoyancy (Hunt, 1990; Osborne and Swarbrick, 1997; Xie et al., 2001; Khoshnaw et al., 2014; Singha and Chatterjee, 2014; Dasgupta et al., 2016). Processes that decrease pore pressure may include uplift-erosion rebound, fluid shrinkage, rock dilation and reservoir depletion (Neuzil, 1993; Hantschel and Kauerauf,

2009; Xu et al., 2012). Overall, there are several key factors that work together causing the appearance of either overpressure or underpressure in subsurface reservoirs.

Table 1 The classification of pore pressure used in this study

Type	Pressure coefficient	Pressure gradient/(MPa·km^{-1})
Underpressure	<0.96	<9.28
Normal pressure	0.96–1.06	9.28–10.41
Overpressure	>1.06	>10.41

Pore pressure plays a significant role in the petroleum and natural gas industry. In coalbed methane (CBM) reservoirs, pore pressure controls the occurrence and content of gases, and further influences CBM production (Yao et al., 2019). Studies on pore pressure can aid in the understanding of fluid pressures in reservoir rocks and operations of lifting fluids from the subsurface (Khoshnaw et al., 2014). More importantly, pore pressure analysis is an essential requirement in any producing sedimentary basin, and is also a fundamental input for successfully carrying out well activities, such as well designs, well abandonment plans, and well service activities in a safe and optimum way (Law and Spencer, 1998; Dasgupta et al., 2016; Saxena et al., 2018). Being unaware of pore pressure in subsurface reservoirs can result in many potentially catastrophic events.

The western Guizhou region, with an estimated CBM resource of 3.15×10^{12} m^3, has the highest potential for commercial CBM exploration and development in South China (Ye et al., 1998; Ju et al., 2018c; Qin et al., 2018). There are generally 10–50 coal seams with varying thicknesses in the most important Permian Longtan coal-bearing formation. These seams can form several superposed CBM-bearing systems vertically with different pore pressures (Chen et al., 2017; Qin et al., 2018). Investigations into the characteristics of pore pressure under these particular geological conditions can provide new geological references for CBM production in this area. Hence, in this study, the main purposes are to analyze the spatial distribution of pore pressure in the CBM reservoirs, and to determine the main geological mechanism for pore pressure differences in coal reservoirs of western Guizhou region, south China.

2 Geological setting

The western Guizhou region in south China is a famous area for commercial CBM exploration and development, in which, the Upper Permian Longtan and Changxing Formations are the main coal-bearing strata. They are characterized by mudstones, sandstones and coal layers interpreted as delta, lagoonal tidal flat and restricted subtidal deposits (Xu and He, 2003; Dou, 2012; Shen et al., 2019). There are generally 10−50 coal seams with varying thicknesses in the Permian Longtan Formation (Fig. 1). The average coal vitrinite reflectance, varying between 0.72% and 3.35%, is dominated by coal burial history and later tectonic thermal events (Xu and He, 2003; Dou, 2012; Li et al., 2015; Tang et al., 2016; Ju et al., 2018c).

After the main coal layers were widely deposited during the Late Permian, the Indosinian, Yanshannian and Himalayan tectonic movements largely destroyed previous coal-accumulating basins in the western Guizhou region (Xu and He, 2003; Li et al., 2015; Ju et al., 2018c). Hence, currently, the majority of Permian coal-bearing strata in the western Guizhou region are only distributed in some residual units, e.g., the Panguan syncline and Santang syncline (Fig. 2).

3 Pore pressure variation

Generally, pore pressure in subsurface formations can be accurately and directly obtained from repeat formation tests (RFTs), drill stem tests (DSTs), or modular dynamic tests (MDTs) (Tingay et al., 2003; Liu et al., 2016). Mud weights (MWs) can also be used as a proxy for pore pressure where direct measurement is not available (Law and Spencer, 1998). For CBM reservoirs, injection-falloff well tests are commonly used to determine pore pressure in coal layers (Chen et al., 2017; Ju et al., 2018a, 2018b, 2019). In this study, 126 injection-falloff and *in-situ* stress well test data were measured from 48 wells in the Permian coal seams of the western Guizhou region (Table 2). Both the pressure gradient and coefficient are calculated for the studied coal layers. The density of pore water is assumed to be 1.00 g/cm^3. Based on these data (Table 2), lateral and vertical variations in pore pressure in different CBM units of the western Guizhou region were analyzed.

3.1 Lateral division of pore pressure zones

In the western Guizhou region, pore pressure in coal reservoirs varies from underpressure to overpressure with a wide range of pressure gradients (3.29−17.11 MPa/km) and pressure coefficient (0.34−1.75) (Table 2). Laterally, five zones can be divided based on pore pressure gradient (or coefficient) in coal reservoirs, namely, the Zhina mining area, southern Liupanshui mining area, northern Liupanshui mining area, northwestern Guizhou mining area, and northern Guizhou mining area. The majority of coal reservoirs in the northern Guizhou (58%) and southern Liupanshui (56%) mining areas are characterized by the presence of overpressure, whereas coal layers in the Zhina (59%), northern Liupanshui (50%), and northwestern Guizhou (100%) mining areas are dominantly underpressure (Table 3).

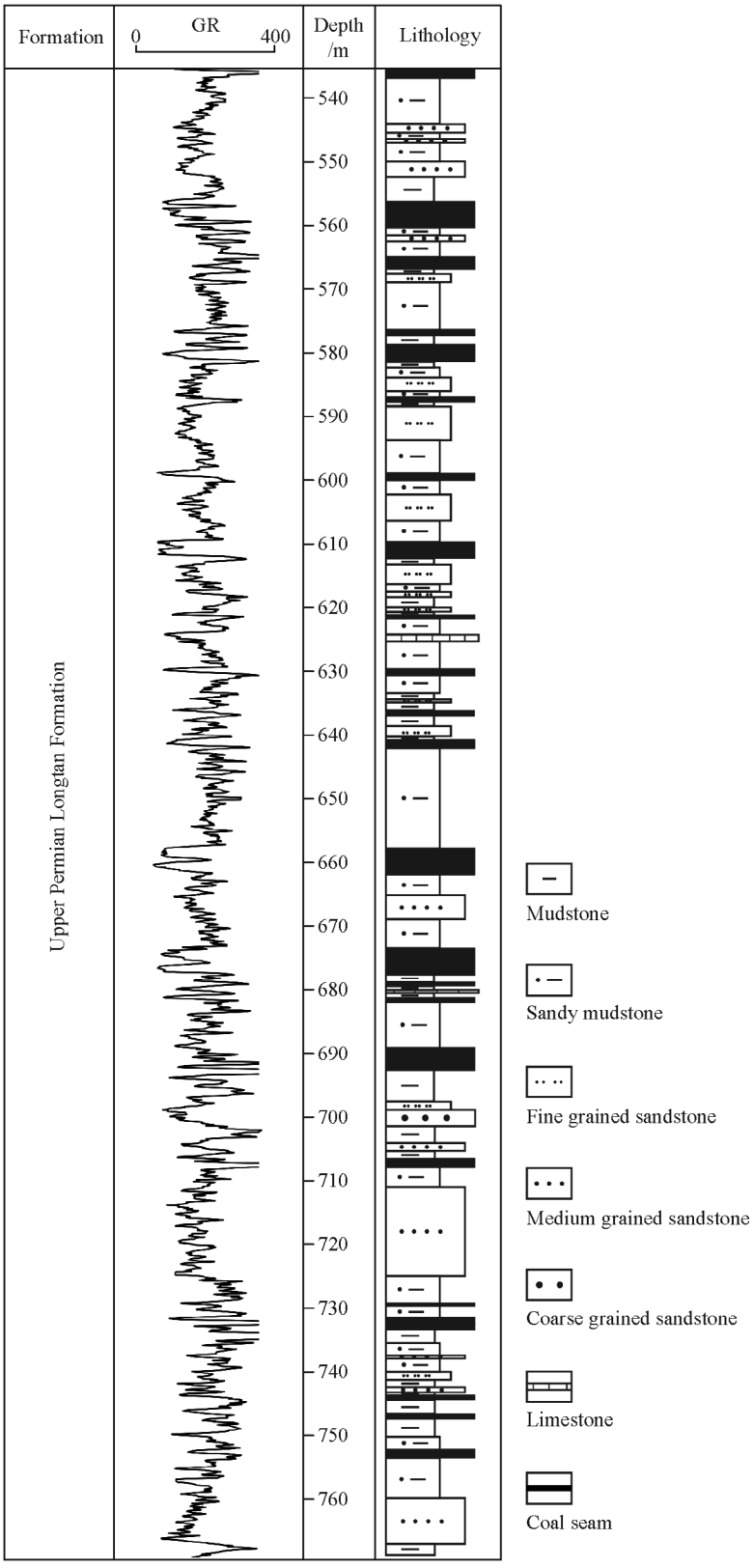

Fig. 1 The Permian Longtan Formation stratigraphy in the western Guizhou region. GR indicates the gamma logging curve, unit: API. The stratigraphy is from Well JV in Panguan syncline.

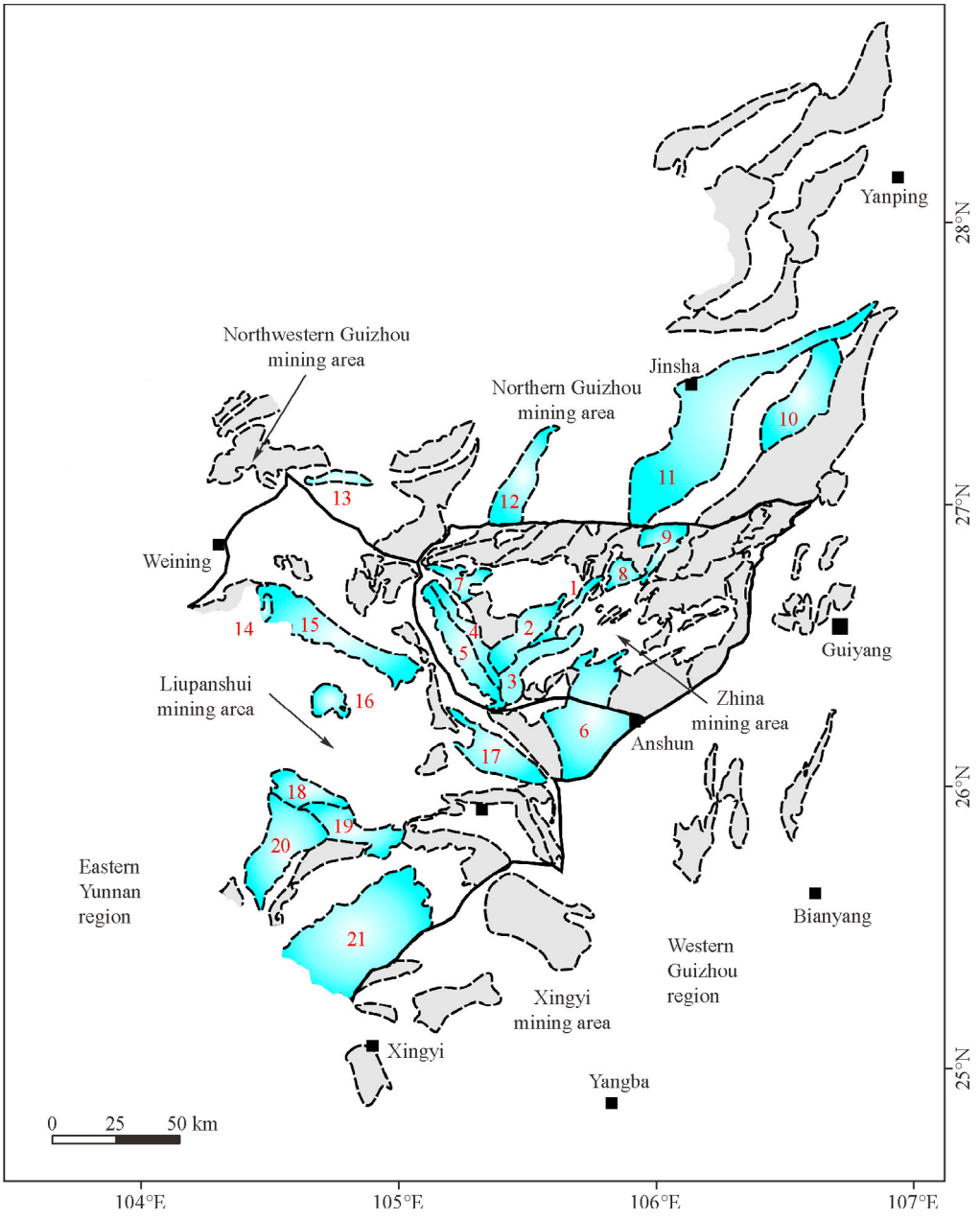

Fig. 2 The distribution of coalbed methane (CBM) units in the western Guizhou region. Grey areas are CBM units in the western Guizhou region, and in this study, pore pressure data are mainly collected from those units with blue color. 1—Agong syncline, 2—Santang syncline, 3—Zhuzang syncline, 4—Jiaga anticline, 5—Bide syncline, 6—Bulang syncline, 7—Bainijing syncline, 8—Guanzhai syncline, 9—Xinpu anticline, 10—Guantian syncline, 11—Jinsha-Qianxi syncline, 12—Luojiaohe syncline, 13—Yemachuan syncline, 14—Gedaying anticline, 15—Gemudi syncline, 16—Yangmeishu syncline, 17—Dailang syncline, 18—Tucheng syncline, 19—Zhaozihe syncline, 20—Panguan syncline, and 21—Qingshan syncline.

3.2 Vertical variation pattern of pore pressure

Observed from a single borehole, the measured magnitudes of pore pressure from deeply buried coal reservoirs are generally higher (Table 2). In this study, the relationship between pore pressure and burial depth of coal seams was analyzed. The result obviously indicates that pore pressure in coal reservoirs linearly increases with burial depth in the western Guizhou region (Fig. 3).

Vertically, in the western Guizhou region, variations in pore pressure in coal reservoirs indicate two different patterns:

Table 2 Parameters from injection-falloff and *in-situ* stress tests in the western Guizhou region

CBM unit	Well	Coal seam number	Depth/m	P_c/MPa	P_o/MPa	Pressure gradient /(MPa·km^{-1})	Pressure coefficient	Permeability /mD
Agong syncline	1#	6	128.18	2.83	0.91	7.10	0.72	0.1800
		27 + 29	312.48	8.07	1.96	6.27	0.64	0.1400
	2#	16	440.70	9.49	4.89	11.10	1.13	0.1700
		30	529.92	12.32	5.09	9.61	0.98	0.0200
Bainijing syncline	3#	5	596.50	7.21	5.48	9.19	0.94	0.5960
		7	630.75	11.20	6.13	9.72	0.99	0.1300
Bide syncline	4#	2	582.98	12.32	6.80	11.66	1.19	0.0700
		6	654.80	14.59	7.33	11.19	1.14	0.3300
	5#	27	375.30	8.37	3.04	8.10	0.83	0.1200
		30	412.83	8.04	4.53	10.97	1.12	0.1200
		32	469.32	7.28	4.73	10.08	1.03	0.5700
	6#	2	520.17	8.90	5.12	9.84	1.00	0.1074
		6	577.76	11.75	5.69	9.85	1.00	0.1682
	7#	2	464.04	8.09	2.97	6.40	0.65	0.5002
		5	502.26	8.75	4.41	8.77	0.90	0.3228
		6	523.35	9.31	4.68	8.93	0.91	0.2999
Bulang syncline	8#	7	200.86	4.31	2.06	10.26	1.05	0.6900
		17	344.78	7.96	3.78	10.96	1.12	0.3300
		18	365.05	8.27	3.93	10.77	1.10	0.5100
		20	380.97	8.51	4.02	10.55	1.08	0.4000
	9#	6_1	269.99	4.25	2.54	9.41	0.96	0.0607
		6_2	280.87	4.25	2.59	9.22	0.94	0.0511
		16	446.90	4.33	4.44	9.94	1.01	0.1287
		27	569.90	8.52	5.25	9.21	0.94	0.0610
Gedaying anticline	10#	3	299.86	6.62	2.79	9.30	0.95	0.1758
		7	362.57	6.73	2.51	6.92	0.71	0.0734
		10	383.68	7.17	2.59	6.75	0.69	0.0928
Guantian syncline	12#	4	463.80	8.01	4.71	10.16	1.04	0.2400
		9	492.85	12.38	4.82	9.78	1.00	0.4300
		13	509.83	11.26	5.18	10.16	1.04	0.7500
		15	549.57	12.35	5.75	10.46	1.07	0.6700

(*Continued*)

CBM unit	Well	Coal seam number	Depth/m	P_c/MPa	P_o/MPa	Pressure gradient /(MPa·km^{-1})	Pressure coefficient	Permeability /mD
Gemudi syncline	13#	7	807.89	9.56	6.43	7.96	0.81	0.0666
		13_2	869.48	13.33	7.06	8.12	0.83	0.2509
Guanzhai syncline	14#	4	555.42	11.60	4.60	8.28	0.85	0.2300
		9	599.74	16.47	5.01	8.35	0.85	0.0210
		11	645.70	16.48	5.20	8.05	0.82	0.0430
Jiaga anticline	15#	3	135.90	2.14	0.78	5.74	0.59	1.5621
		4	142.78	2.40	0.81	5.67	0.58	1.3103
Langdai syncline	16#	7	94.38	2.19	0.66	6.99	0.71	0.6700
		15	247.65	5.17	1.64	6.62	0.68	0.1820
		18	298.45	5.33	2.06	6.90	0.70	0.5600
Luojiaohe syncline	17#	18	296.43	4.82	2.71	9.14	0.93	0.5070
		29	321.96	9.14	4.56	14.16	1.45	0.0088
		51	368.69	12.58	6.31	17.11	1.75	0.0638
		73	439.51	11.42	6.51	14.81	1.51	0.0706
		78	464.27	11.56	5.36	11.55	1.18	0.0391
Panguan syncline	18#	6_1	674.45	10.37	6.26	9.28	0.95	0.1920
		12	722.09	12.17	6.32	8.75	0.89	0.5730
		18	774.39	12.18	6.96	8.99	0.92	0.0492
		24	832.89	13.57	10.83	13.00	1.33	0.0578
	19#	7	554.24	15.68	6.54	11.80	1.20	0.4260
	20#	3	359.09	10.40	3.95	11.00	1.12	0.0173
		9	408.53	13.33	5.27	12.90	1.32	0.0044
	21#	3	558.05	10.23	5.66	10.13	1.03	0.3240
		10	611.10	12.80	6.00	9.82	1.00	0.0975
		13	641.58	15.79	6.14	9.57	0.98	0.0157
		22	706.93	11.85	7.04	9.96	1.02	0.3130
	22#	1	439.67	4.84	4.75	10.81	1.10	0.4930
		16_1	566.96	9.10	6.01	10.60	1.08	0.1550
		20_2	603.37	12.56	6.03	9.99	1.02	0.1310
		22	631.65	9.81	6.70	10.61	1.08	0.0759
	23#	12	1133.90	27.21	12.89	11.37	1.16	0.0010
		24	1243.60	27.36	11.28	9.07	0.93	0.0060

(*Continued*)

CBM unit	Well	Coal seam number	Depth/m	P_c/MPa	P_o/MPa	Pressure gradient /(MPa·km^{-1})	Pressure coefficient	Permeability /mD
	24#	15	1080.00	23.76	12.28	11.37	1.16	0.0096
	25#	10	1139.70	23.93	10.13	8.89	0.91	0.0020
Jinsha-Qianxi syncline	26#	9	251.83	3.82	2.62	10.40	1.06	0.6100
		15	376.40	6.35	3.57	9.48	0.97	0.4300
		4	338.07	7.02	4.47	13.22	1.35	0.0874
	27#	9	352.12	8.56	3.70	10.51	1.07	0.0758
		15	408.16	11.19	6.45	15.80	1.61	0.0025
	28#	4	435.10	8.76	3.79	8.71	0.89	0.0907
	29#	4	890.41	12.41	8.04	9.03	0.92	0.0268
		15	964.82	17.52	8.11	8.41	0.86	0.0276
	30#	12	1023.50	18.46	12.63	12.34	1.26	0.0700
		16	1096.70	17.68	12.81	11.68	1.19	0.0600
Qingshan syncline		17	147.17	2.39	1.20	8.15	0.83	0.2700
	31#	19	175.30	3.60	1.51	8.61	0.88	0.2560
		27	323.30	5.19	2.95	9.12	0.93	0.5600
	32#	18	341.95	8.20	3.93	11.49	1.17	0.0007
		19	367.09	11.01	4.11	11.20	1.14	0.0002
	33#	19	493.29	11.53	4.09	8.29	0.85	0.0110
		26	628.61	11.53	6.37	10.13	1.03	0.2010
		3	647.82	14.80	10.35	15.98	1.63	0.0002
		9	712.62	12.80	8.66	12.15	1.24	0.0081
	34#	12	726.63	14.22	9.37	12.90	1.32	0.0106
		17_1	742.84	18.14	8.97	12.08	1.23	0.0027
		17_2	752.04	14.18	7.40	9.84	1.00	0.0109
		19	771.73	12.86	8.86	11.48	1.17	0.0074
		17	292.22	6.28	3.54	12.11	1.24	0.0078
	35#	19	329.40	8.29	3.66	11.11	1.13	0.0110
		29	426.95	9.56	4.57	10.70	1.09	0.0130
	36#	17	632.36	7.14	5.50	8.70	0.89	0.4800
		19	665.02	15.12	7.51	11.29	1.15	0.0620
Santang syncline	37#	6	220.77	5.04	1.04	4.71	0.48	0.0100
		16	325.29	5.41	3.43	10.54	1.08	0.0314
		27	399.94	6.63	2.24	5.60	0.57	0.0857

(*Continued*)

CBM unit	Well	Coal seam number	Depth/m	P_c/MPa	P_o/MPa	Pressure gradient /(MPa·km^{-1})	Pressure coefficient	Permeability /mD
Tucheng syncline	38#	1 + 3	619.26	10.67	6.94	11.21	1.14	0.1060
		9	661.23	11.11	7.02	10.61	1.08	0.0934
		16	738.90	13.14	10.11	13.69	1.40	0.2100
		27_1	920.03	21.01	12.35	13.42	1.37	0.0437
Xinpu anticline	39#	18	191.95	4.52	2.08	10.84	1.11	0.0052
		20	215.25	7.19	2.29	10.64	1.09	0.0133
Yangmeishu syncline	40#	5_2	580.00	8.35	6.95	11.99	1.22	0.0661
		7	630.00	10.85	6.25	9.92	1.01	0.1730
		23_2	806.00	14.92	7.62	9.45	0.96	0.1310
Zhaozihe syncline	41#	3	31.77	1.85	0.52	16.37	1.67	0.6600
		12	195.91	3.73	2.16	11.03	1.13	0.2000
		17	238.29	4.82	2.32	9.74	0.99	0.2100
		19	270.50	5.77	2.60	9.61	0.99	0.6100
		28	437.41	10.15	4.74	10.84	1.11	0.5700
		29	461.18	10.34	5.04	10.93	1.11	0.0700
Yemachuan syncline	42#	1	751.20	8.17	5.16	6.87	0.70	0.0347
		4	795.70	11.63	5.46	6.86	0.70	0.0319
		7	826.90	13.76	5.54	6.70	0.68	0.0291
	43#	1	659.98	7.48	3.44	5.21	0.53	0.0363
		5	728.54	9.61	3.10	4.26	0.43	0.0830
	44#	13	438.31	7.37	2.78	6.34	0.65	0.0738
		18	441.98	6.57	3.17	7.17	0.73	0.1033
	45#	2	418.65	6.93	1.58	3.77	0.39	0.0763
		3	428.57	6.97	1.97	4.60	0.47	0.0656
		5	450.37	6.00	1.48	3.29	0.34	0.1210
		8	469.96	6.31	1.68	3.57	0.36	0.0585
	46#	4	455.92	7.13	1.97	4.32	0.44	0.0830
Zhuzang syncline	47#	16	379.70	8.01	2.95	7.77	0.79	0.0179
		23	431.38	15.59	3.04	7.05	0.72	0.0002
	48#	16	736.98	17.56	6.86	9.31	0.95	0.0005

Notes: In this table, P_c is fracture closing pressure, and P_o is pore pressure.

Table 3 Zone divisions based on pore pressure gradient or coefficient in coal reservoirs of western Guizhou region

Zone	CBM unit	Pressure gradient/(MPa·km^{-1}) min–max	Pressure coefficient min–max	Number of underpressure layer	Number of normal pressure layer	Number of overpressure layer
Northern Guizhou mining area	Guantian syncline	9.78–10.46	1.00–1.07	0	3	1
	Jinsha-Qianxi syncline	8.41–15.80	0.86–1.61	3	1	6
	Luojiaohe syncline	9.14–17.11	0.93–1.75	1	0	4
	total			4	4	11
Zhina mining area	Guanzhai syncline	8.05–8.35	0.82–0.85	3	0	0
	Xinpu anticline	10.64–10.84	1.09–1.11	0	0	2
	Agong syncline	6.27–11.10	0.64–1.13	2	1	1
	Bainijing syncline	9.19–9.72	0.94–0.99	1	1	0
	Santang syncline	4.71–10.54	0.48–1.08	2	0	1
	Zhuzang syncline	7.05–9.31	0.72–0.95	3	0	0
	Jiaga anticline	5.67–5.74	0.58–0.59	2	0	0
	Bide syncline	6.40–11.66	0.65–1.19	4	3	3
	total			17	5	7
Northern Liupanshui mining area	Bulang syncline	9.21–10.96	0.94–1.12	0	4	4
	Langdai syncline	6.62–6.99	0.68–0.71	3	0	0
	Gedaying anticline	6.75–9.30	0.69–0.95	3	0	0
	Gemudi syncline	7.96–8.12	0.81–0.83	2	0	0
	total			8	4	4
Southern Liupanshui mining area	Yangmeishu syncline	9.45–11.99	0.96–1.22	0	2	1
	Tucheng syncline	10.61–13.69	1.08–1.40	0	0	4
	Zhaozihe syncline	9.61–16.37	0.98–1.67	0	2	4
	Panguan syncline	8.75–13.01	0.89–1.33	5	5	9
	Qingshan syncline	8.15–15.98	0.83–1.63	5	2	11
	total			10	11	29
Northwestern Guizhou mining area	Yemachuan syncline	3.29–7.17	0.34–0.73	12	0	0
	total			12	0	0

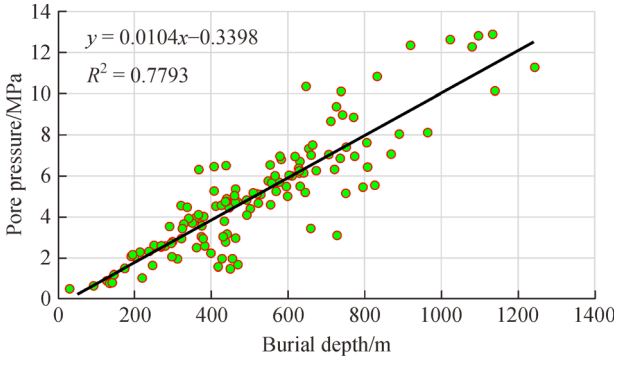

Fig. 3 The relationship between pore pressure and burial depth in the western Guizhou region. Here, y indicates pore pressure in coal reservoirs, x is burial depth, and R is the correlation coefficient.

1) The pore pressure gradient (or pressure coefficient) is nearly the same in different coal reservoirs, e.g., wells #6, #8, #9, #14 and #16 (Table 2).

2) The pore pressure gradient (or pressure coefficient) has cyclic variation in a borehole profile with multiple coal seams, e.g., wells #17, #34 and #41 (Table 2).

Commonly, in a gas-bearing system, fluids among different coal reservoirs are connected, and this fluid connection can be recognized by the vertical distribution of the pore pressure gradient or coefficient (Qin et al., 2008); namely, the difference in the pore pressure gradient or coefficient is extremely low among different coal reservoirs. In wells #17, #34 and #41 of the western Guizhou region, the pore pressure difference is high among coal reservoirs, and it can be deduced that there is no fluid connection and that there are multiple independent gas-bearing systems vertically. Hence, here, a vertical overlap

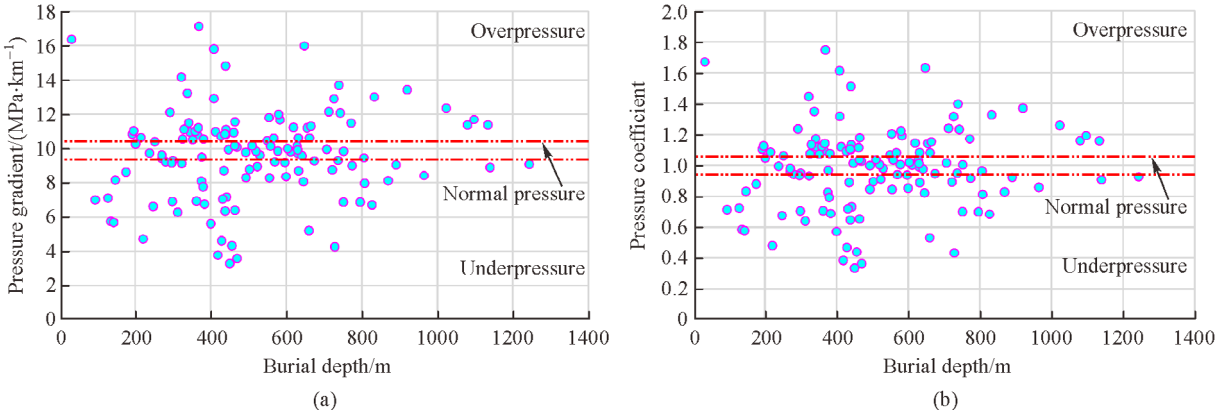

Fig. 4 Variations of (a) pore pressure gradient and (b) pressure coefficient in coal reservoirs with burial depth in the western Guizhou region.

of multiple independent CBM systems can be referred to as a "superimposed CBM system" (Qin et al., 2008, 2018). As a result, both the pressure gradient and coefficient have no obvious relationships with burial depth in the western Guizhou region (Fig. 4).

4 Factors for pore pressure differences

Several factors can cause the pore pressure to be higher or lower than the hydrostatic pressure in subsurface reservoirs (Neuzil, 1993; Osborne and Swarbrick, 1997; Wu, 2005; Hantschel and Kauerauf, 2009; Xu et al., 2011; Dasgupta et al., 2016; Fu et al., 2020). Regarding pore pressure in coal reservoirs, Wu et al. (2014) suggested that tectonic activities, hydrocarbon generation, and roof sealing conditions were the main factors affecting overpressure. Factors including tectonic uplift, relatively low stress magnitude, hydrocarbon generation cessation, and simple hydrogeological conditions can result in underpressure in coal reservoirs (Wu, 2005; Yao et al., 2019). Xu et al. (2011) indicated that the present-day *in-situ* stress field and coal permeability were the main factors affecting lateral pore pressure differences. Hence, in this study, factors including the present-day stress field, coal permeability, thermal evolution stage, hydrocarbon generation, basement structure and tectonic activity, and sealing capacity were analyzed to determine the mechanisms for pore pressure differences in the western Guizhou region.

4.1 Present-day *in-situ* stress field

In general, the pore pressure and *in-situ* stress field are interrelated (Fu et al., 2020). Pore pressure is an important component of the stress tensor and is required to calculate stress magnitudes (Liu et al., 2016; Ju et al., 2017, 2019). The spatial-temporal changes in horizontal minimum principal stress are a function of the pore pressure changes, and this observed phenomenon is termed "pore pressure/stress coupling" (Engelder and Fischer, 1994; Tingay et al., 2003; Liu et al., 2016).

Commonly, based on ground vertical drilling hydraulic fracturing measurements, the horizontal minimum principal stress (S_{hmin}) is considered to be equal to the shut-in pressure (P_c) (Haimson and Cornet, 2003).

$$S_{hmin} = P_c \tag{1}$$

where S_{hmin} is the horizontal minimum principal stress, MPa, P_c is fracture closing pressure, MPa.

Based on the measured data in Table 2, the relationship between pore pressure and S_{hmin} in coal seams of the western Guizhou region was analyzed, and the result indicates that pore pressure linearly increases with S_{hmin} (Fig. 5). However, the relationship between the pressure

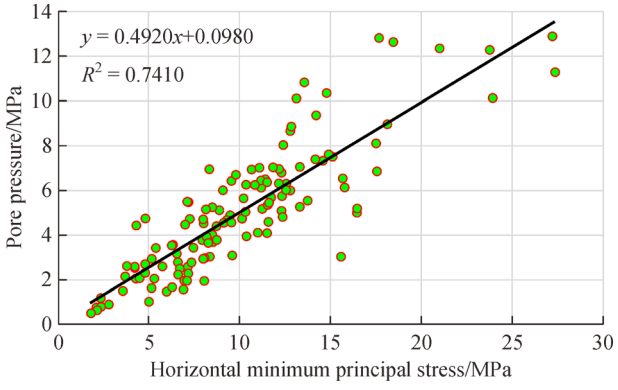

Fig. 5 The relationship between pore pressure and hori-zontal minimum principal stress in coal reservoirs of western Guizhou region. Here, y is pore pressure, MPa; x is horizontal minimum principal stress, MPa; R is correlation coefficient.

gradient (or coefficient) and burial depth displays a different pattern in the study area (Fig. 6). Generally, at a relatively low S_{hmin} magnitude (less than approximately 10 MPa), both the pore pressure gradient and coefficient increase with increasing S_{hmin} magnitude; whereas they are nearly unchanged when the S_{hmin} magnitude is greater than approximately 10 MPa (Fig. 6).

In the western Guizhou region, the present-day *in-situ* stress magnitudes are relatively higher in the northern Guizhou and southern Liupanshui mining areas, and relatively lower in the northwestern Guizhou, northern Liupanshui and Zhina mining areas (Fig. 7). Hence, the

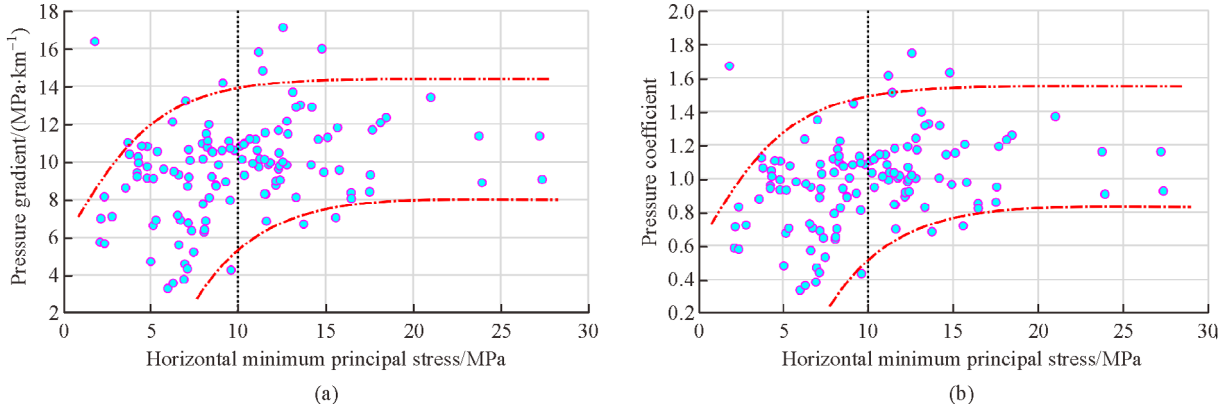

Fig. 6 Variations of (a) pore pressure gradient and (b) pressure coefficient in coal reservoirs with horizontal minimum principal stress in the western Guizhou region.

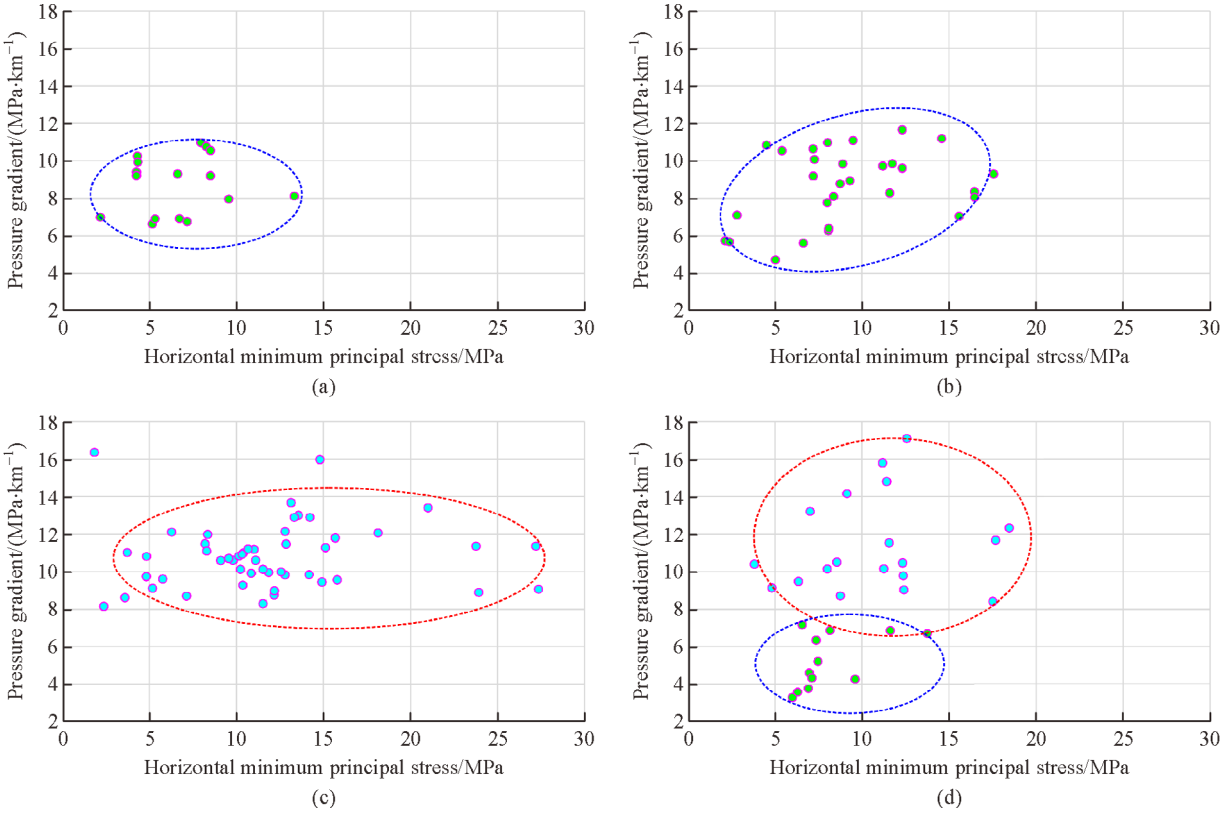

Fig. 7 Variations of pore pressure gradient with horizontal minimum principal stress in different mining areas of western Guizhou region. (a) Northern Liupanshui mining area, (b) Zhina mining area, (c) southern Liupanshui mining area, and (d) northern and northwestern Guizhou mining area.

present-day *in-situ* stress field may be an important factor influencing the lateral division of pore pressure zones, especially for the southern and northern Liupanshui mining areas (Figs. 7(a) and 7(c)).

4.2 Coal permeability

The permeability is an important parameter indicating the fluid flow ability in coal reservoirs (Chen et al., 2017; Ju et al., 2018b, 2018c), which may influence pore pressure distribution (Xu et al., 2011). The relationship between pore pressure and coal permeability indicates that, in the western Guizhou region, as coal permeability increases, pore pressure decreases sharply at the initial stage and gently in the subsequent stage (Fig. 8). The variation in the pore pressure gradient (or coefficient) with coal permeability indicates that all three types of pore pressure (underpressure, normal pressure and overpressure) may appear when coal permeability is relatively low, which is generally less than 0.2 mD in this study. When the permeability increases, normal pressure becomes the dominant type in coal reservoirs of western Guizhou region (Fig. 9).

In the western Guizhou region, the majority of coal reservoirs in all divided four mining areas are characterized by low permeability (Fig. 10). However, as mentioned above, pore pressure in coal reservoirs can be classified as underpressure, normal pressure and overpressure under low-permeability conditions. Hence, the results indicate that coal permeability may not be a critical factor for pore pressure differences in the study area.

4.3 Thermal evolution stage

The Zhina (underpressure) and southern Liupanshui (overpressure) mining areas are taken as examples in this study. The measured homogenization temperatures in the western Guizhou region indicate that there are two major thermal evolution stages (Table 4; Xu and He, 2003; Tang et al., 2016): i) the temperature of the first stage is 115°C−192°C in the Zhina mining area and 65°C−119°C in the southern Liupanshui mining area, which is mainly caused by the metamorphism of coal seams; ii) the temperature of the second stage is 206°C−244°C and 135°C−150°C in the Zhina and southern Liupanshui mining areas, respectively, which may result from later tectonic-thermal events, e.g., the intrusion of mantle derived magmatic hydrothermal fluid (Table 4; Dou, 2012; Tang et al., 2016).

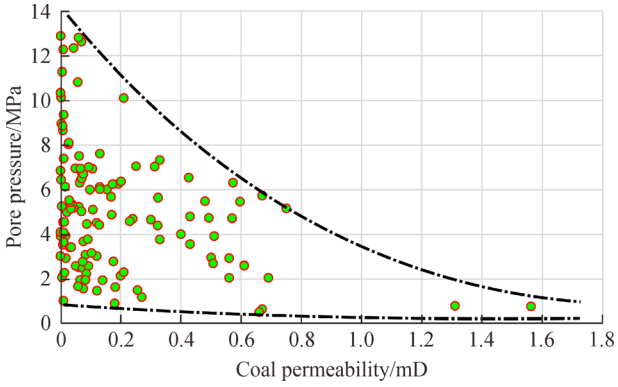

Fig. 8 The relationship between pore pressure and coal permeability in the western Guizhou region.

Dou (2012) studied the burial history and thermal evolution in different CBM units of the western Guizhou region. The Santang syncline (Zhina mining area; underpressure) and Panguan syncline (southern Liupanshui mining area; overpressure) were selected for comparative analysis. The results indicated that in the western Santang syncline, coal seams entered the mature (early and middle) stage in the Early Triassic, mature (late) stage in the Middle Triassic, and the high and over mature stage in the Middle Jurassic (Fig. 11(a)). In the western Panguan syncline, coal seams entered the mature (early) stage in the Early Triassic, mature (middle) stage in the Middle Jurassic, and mature

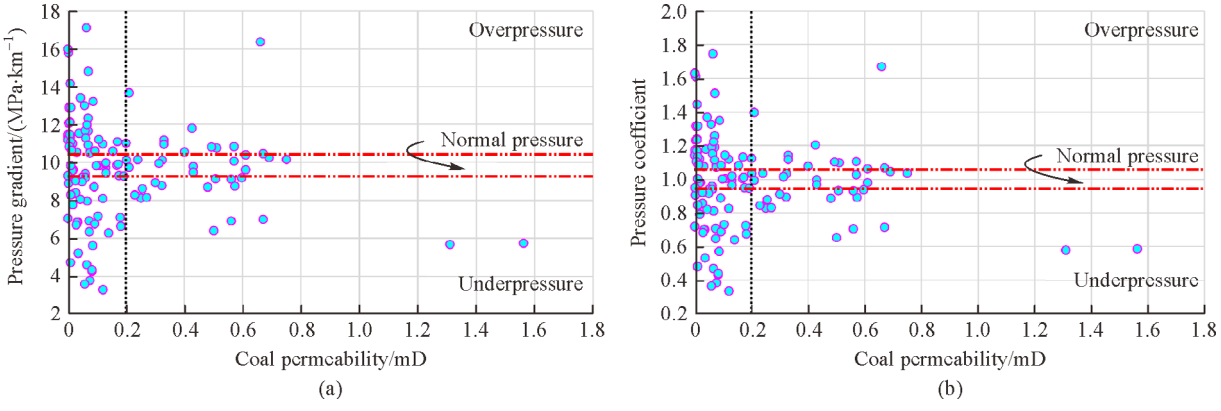

Fig. 9 Variations of (a) pore pressure gradient and (b) pressure coefficient with coal permeability in the western Guizhou region.

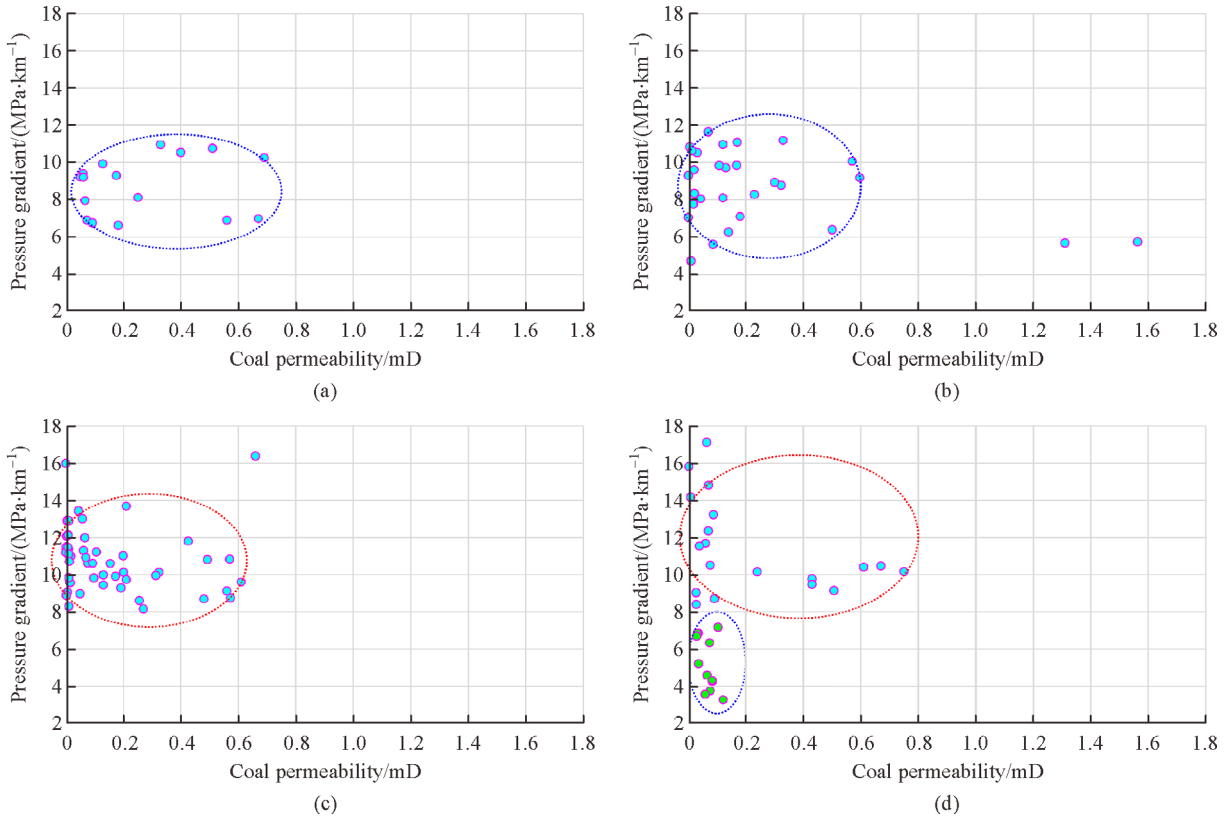

Fig. 10 Variations of pore pressure gradient with coal permeability in different mining areas of western Guizhou region. (a) Northern Liupanshui mining area, (b) Zhina mining area, (c) southern Liupanshui mining area, and (d) northern and northwestern Guizhou mining area.

Table 4 Measured the maximum vitrinite reflectance and homogenization temperature of inclusion (after Tang et al., 2016)

Zone	Maximum vitrinite reflectance R_o/%	Homogenization temperature of inclusion/°C		
		Range	First stage	Second stage
Zhina mining area	1.64–3.35	115–244	115–192	206–244
Southern Liupanshui mining area	0.72–1.27	65–150	65–119	135–150

(late) stage in the Early Cretaceous (Fig. 11(b)).

Overall, in the western Guizhou region, the maximum vitrinite reflectance (R_o) ranges from approximately 0.72% to 3.35% after two major thermal evolution stages (Fig. 12; Xu and He, 2003; Tang et al., 2016). The spatial distribution of the thermal evolution stage has no obvious relationship with pore pressure in coal reservoirs. Both the northern Guizhou and southern Liupanshui mining areas are characterized by dominant overpressure in coal reservoirs; however, the R_o values are high (1.7%−3.0%) in the northern Guizhou mining area and low (0.9%−1.9%) in the southern Liupanshui mining area. Hence, the results indicate that the thermal evolution stage of coal seams contributes little to pore pressure differences in the western Guizhou region.

4.4 Hydrocarbon generation

Based on the burial history and thermal evolution in the Santang and Panguan synclines (Fig. 11), hydrocarbon generation is analyzed. In the Santang syncline (under-pressure), three stages of hydrocarbon generation can be delineated: i) in the Middle Triassic, the temperature was approximately 140°C, the R_o values were 1.0%−1.2%, and the coal seams evolved into the fat coal stage; ii) in the Middle-Late Jurassic, the temperature was nearly 160°C, the Ro values were 1.2%−1.5%, and the coal seams evolved into the cooking coal stage; iii) due to the tectonic-thermal events in the Early Cretaceous, the temperature quickly increased to 220°C, the Ro values were 2.6%−3.5%, and the coal seams evolved into the anthracite stage.

In the Panguan syncline (overpressure), there are also three stages of hydrocarbon generation: i) in the Middle Triassic, the temperature was approximately 90°C, the R_o values were 0.5%−0.6%, and the coal seams evolved into the long flame coal stage; ii) in the Middle Jurassic, the temperature was nearly 110°C, the R_o values were 0.7%−0.8%, and the coal seams evolved into the gas coal stage; iii) due to the tectonic-thermal events in the Early Cretaceous, the temperature quickly increased to 140°C, the R_o values were 0.9%−1.2%, and the coal seams evolved into the fat coal stage.

Coal seams in the Santang syncline are buried much deeper than those in the Panguan syncline, which may influence their thermal evolution. However, nearly all coal seams in the western Guizhou region can evolve into the mature stage (late; R_o: 1.0%−1.3%) (Figs. 11 and 12). Thermal simulation experiments indicate that the majority of CBM in coal seams is formed during the fat to meager coal stage (R_o: 1.00%−1.75%) with its R_o peak of approximately 1.3% (Fig. 13; Wu, 2005; Thakur et al., 2014). Hence, in the western Guizhou region, large amounts of CBM were generated during the Yanshanian. The produced CBM volume is much larger than the volume that can be absorbed by coal seams, which results in the widely distributed overpressure in coal reservoirs during the Yanshanian. However, the current pore pressure difference in different geological units and burial depths may be influenced by other factors.

4.5 Basement structure and tectonic activity

Basement structure and tectonic activity factors are significant in influencing pore pressure variation in coal reservoirs. The characteristics of basement structure may cause differential development of sedimentation, magmatism, metamorphism and tectonic deformation in a sedimentary basin. Based on the characteristics of the regional gravity anomaly in the western Guizhou region, the distribution of the basement structure is shown in Fig. 14. Obviously, coal reservoirs in areas with NW-SE-trending basement faults (e.g., Gemudi and Dailang synclines) are generally characterized by underpressure, which suggests that the NW-SE-trending basement faults in the northern Liupanshui mining area may cause the appearance of underpressure in coal reservoirs.

The western Guizhou region experienced Indosinian, Yanshannian and Himalayan tectonic movements after the main coal layers were deposited in the Late Permian (Xu and He, 2003; Dou, 2012; Li et al., 2015; Ju et al., 2018c). Among these movements, Yanshannian tectonic activities are extremely critical for the deformation and structural patterns in the western Guizhou region. During the Yanshannian, the evolution of the tectonic stress field was as follows: i) NE-SW-trending compression, ii) nearly N-S-trending compression, iii) NW-SE-trending compression, and iv) regional extension (Dou, 2012). The stress field sequence further explains the appearance of underpressure in areas with NW-SE-trending basement faults, where NW-SE-trending compression occurred after NE-SW-trending compression and parallel to the dominant basement structures. In addition, large numbers of faults (especially normal faults) are developed in the Zhina mining area (Fig. 15), which are typically generated from structural inversion caused by the rapid uplift of Xuefeng Mountain. The Zhina mining area is close to Xuefeng Mountain, hence, the strength of regional extension is higher than the other areas, generating more normal faults in this area (Qiu et al., 1999; Xu and He, 2003; Dou, 2012).

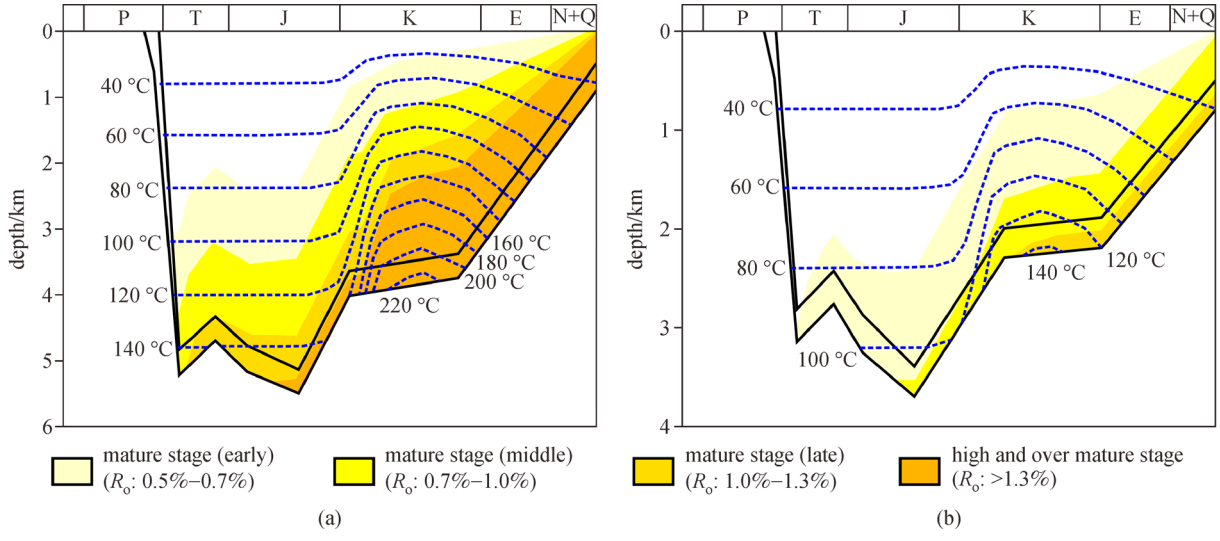

Fig. 11 Burial history and thermal evolution of coal seam in western Santang syncline (Zhina mining area); (a) and western Panguan syncline (southern Liupanshui mining area); (b) of western Guizhou region (after Dou, 2012).

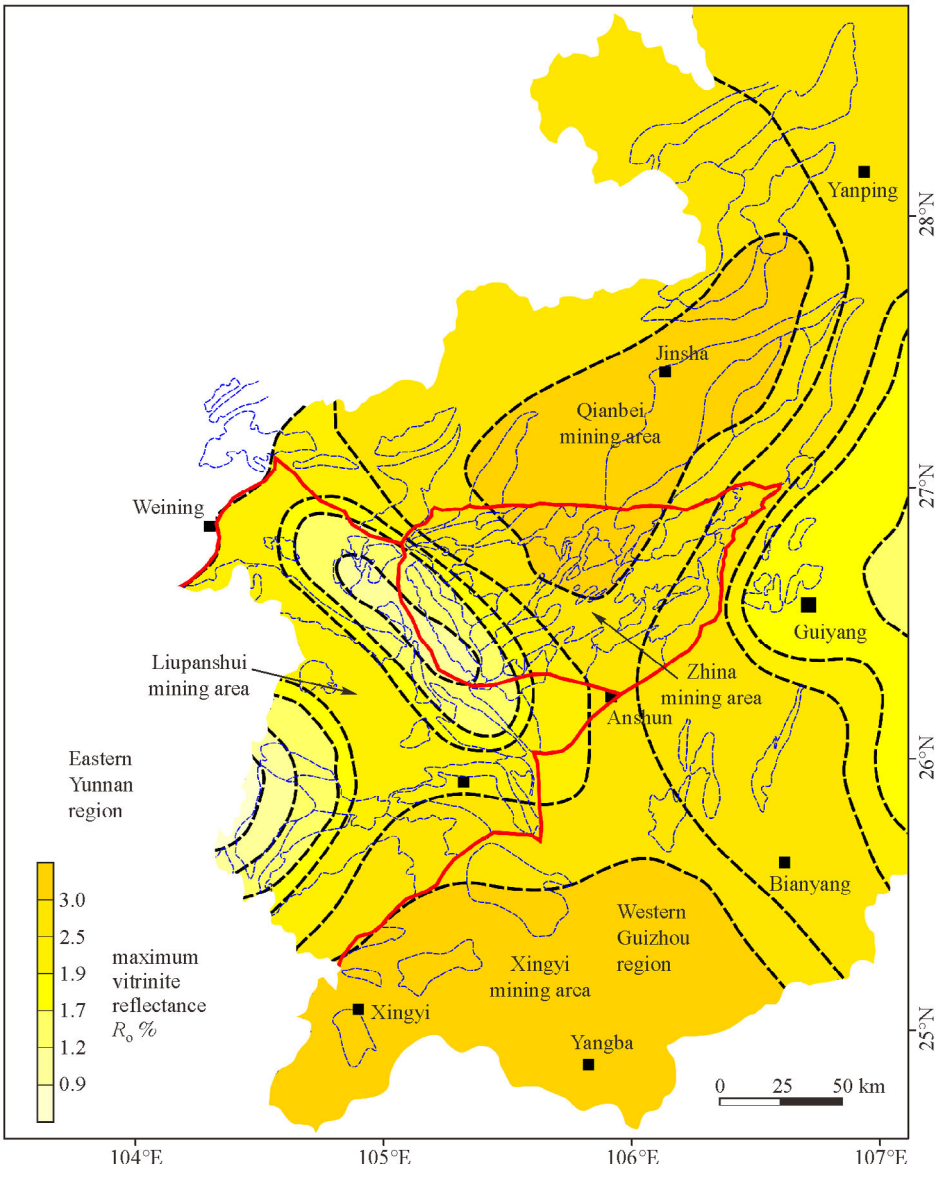

Fig. 12 Isoline map showing the maximum vitrinite reflectance in the Permian coal reservoirs of western Guizhou region (the data are from Xu and He, 2003).

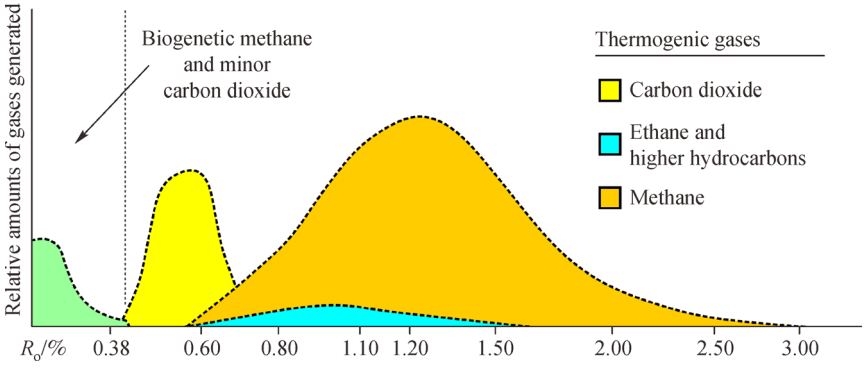

Fig. 13 Generation of thermogenic gas from coal with increasing thermal maturity (after Thakur et al., 2014).

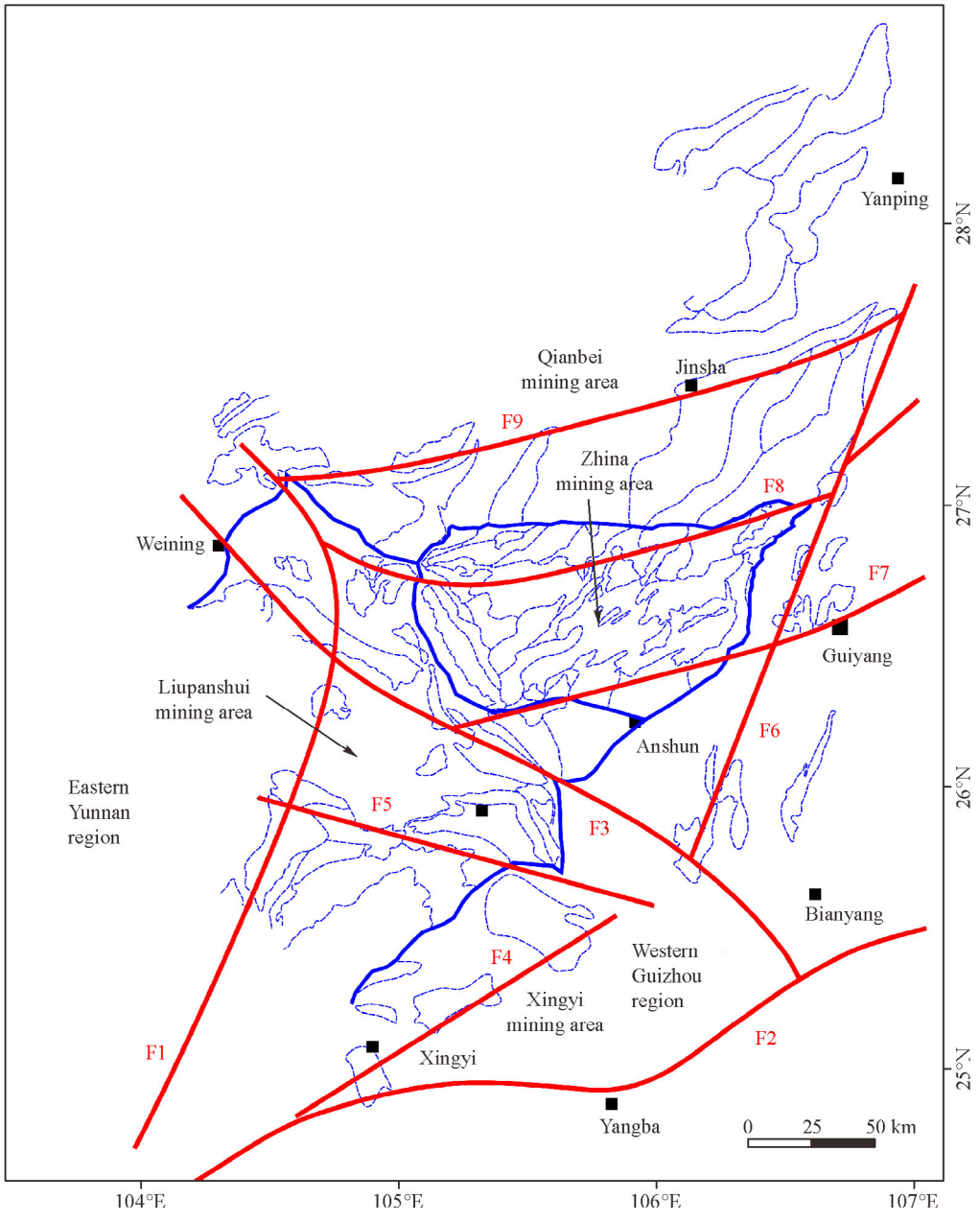

Fig. 14 The distribution of basement structure in the western Guizhou region (after Dou, 2012). F1: Panxian-Shuicheng Fault, F2: South Panjiang Fault, F3: Shuicheng-Ziyun Fault, F4: South Xingyi-Anlong Fault, F5: Puan Fault, F6: Zunyi-Pingba Fault, F7: Guiyang-Puding Fault, F8: Qianzhong Fault, and F9: Hezhang-Jinsha Fault.

The development of normal faults in the Zhina mining area produces an open environment that favors the formation of underpressure in coal reservoirs.

Hence, in the western Guizhou region, from coal reservoirs with overpressure in the Yanshanian to the current appearance of underpressure, normal pressure and overpressure in different CBM units and coal seams, the basement structure and tectonic activity may play important roles in the differential development of pore pressure in coal reservoirs.

4.6 Sealing capacity

The sealing capacity of caprocks is significant for analyzing fluid connections between two coal reservoirs. Generally, in the western Guizhou region, the caprocks are mainly mudstones and silty mudstones (Fig. 1). The sealing capacity of siderite-bearing mudstone is generally larger than that of siderite-free mudstone (Shen et al., 2019). Hence, siderite-bearing strata with low permeability and porosity have been considered the most significant gas

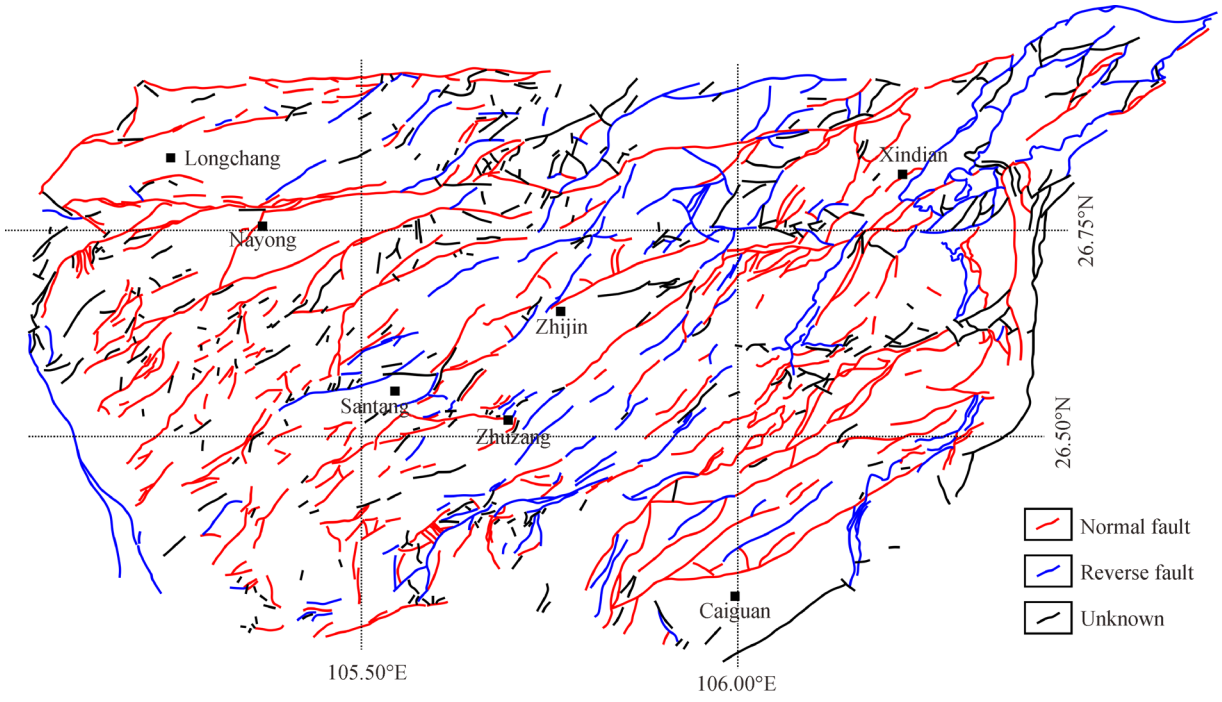

Fig. 15 The development and type of faults in the Zhina mining area of western Guizhou region.

barrier layers (Qin et al., 2008, 2018; Shen et al., 2019). Siderite can use its sealing capacity during the entire gas accumulation process and control the distribution of CBM reservoirs.

In this study, based on sequence stratigraphy, the development of siderite-bearing strata, wavelet analysis, gas content and breakthrough pressure, multiple superposed gas-bearing systems are divided with an example of Well #18 in Panguan syncline (Fig. 16). In this well, well tests were carried out in coal seams 6_1, 12, 18 and 24. Coal seam 6_1 is in the first gas-bearing system with a pore pressure gradient of 9.28 MPa/km. Coal seams 12 and 18 are in the second gas-bearing system, and their pore pressure gradients are 8.75 MPa/km and 8.99 MPa/km, respectively. Coal seam 24 is in the third gas-bearing system with pore pressure gradient of 13.01 MPa/km (Fig. 16 and Table 2). Hence, the development of siderite-bearing strata importantly prevents fluid connections among different coal reservoirs, causing vertical differential pore pressure gradients.

Overall, based on the above analysis, in the western Guizhou region, the present-day *in-situ* stress field, basement structure and tectonic activity may act as the most important factors for the lateral pore pressure difference in coal reservoirs. The sealing capacity of caprocks and the present-day *in-situ* stress field in coal reservoirs may control the vertical pore pressure difference. Factors including coal permeability, thermal evolution and hydrocarbon generation contribute little to the pore pressure distribution of coal reservoirs. Actually, the current development characteristics of pore pressure in different geological units and burial depths of the western Guizhou region result from many factors that work together.

In addition, the western Guizhou region is a large area, which includes many different CBM reservoirs, and each reservoir has its special features. In this study, we focus on the mechanism of pore pressure variation in multiple coal reservoirs in the western Guizhou region on a regional scale. The controlling factors for pore pressure variation in a single syncline may differ from each other, which requires further analysis.

5 Conclusions

In this study, the spatial distribution of pore pressure in CBM reservoirs is analyzed, and the main geological mechanism for pore pressure differences in coal reservoirs of the western Guizhou region is determined.

1) The western Guizhou region can be divided into five lateral zones based on the pore pressure gradient and/or coefficient of coal reservoirs: the Zhina, northern Liupanshui, southern Liupanshui, northern Guizhou, and northwestern Guizhou mining areas. The Zhina, northwestern Guizhou, and northern Liupanshui mining areas are characterized by underpressure, whereas coal reservoirs in the northern Guizhou and southern Liupanshui mining areas are mainly characterized by overpressure.

2) Vertically, in the western Guizhou region, variations in the pore pressure in coal reservoirs indicate two basic patterns: i) the pore pressure gradient (or pressure

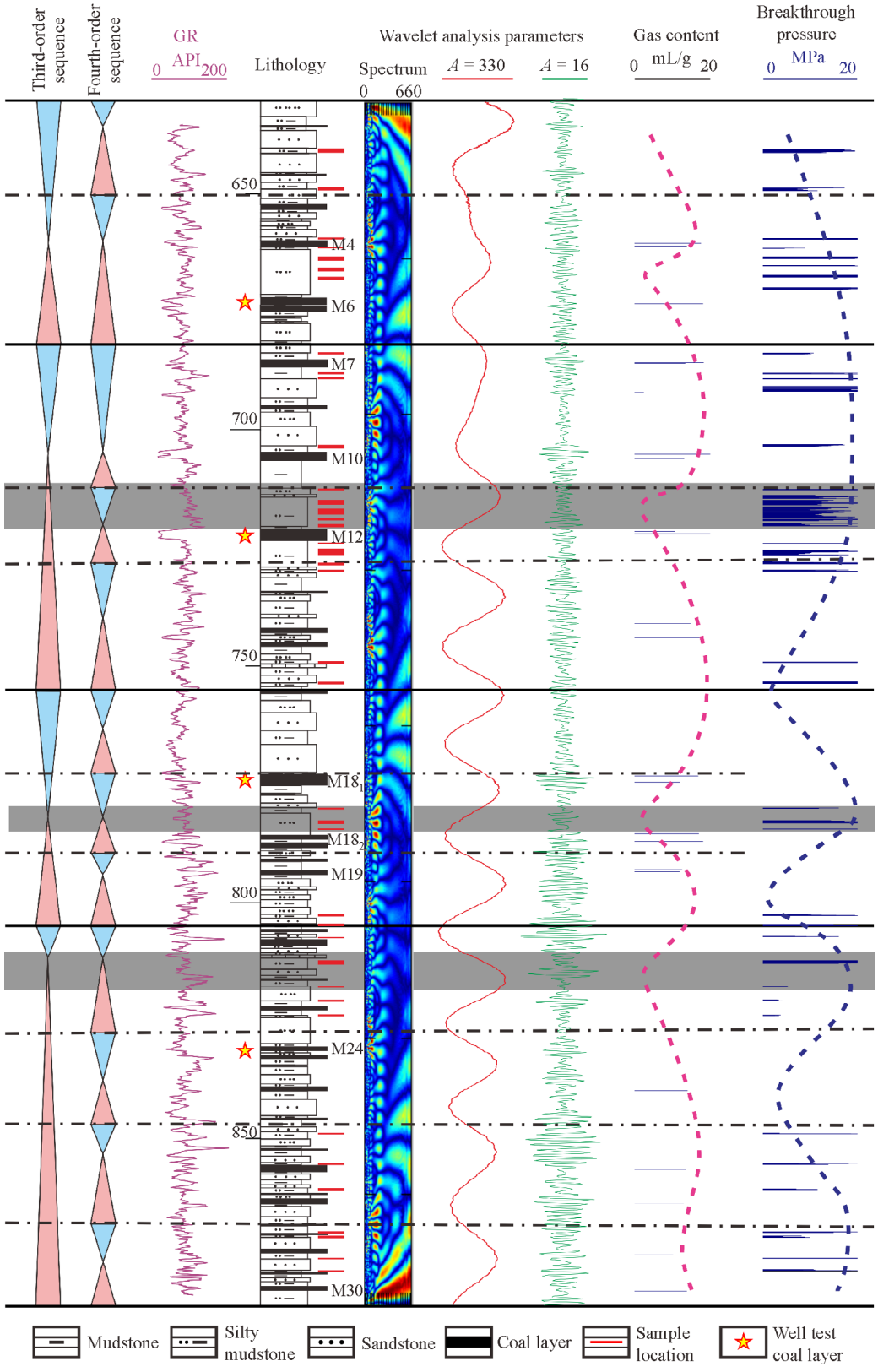

Fig. 16 The division of multiple superposed gas-bearing systems in Well 18 of Panguan syncline. The gray bands are indicative of siderite-bearing strata.

coefficient) is nearly the same in different coal reservoirs, and ii) pore pressure gradient (or coefficient) varies cyclically in a borehole profile with multiple coal seams.

3) Factors including coal permeability, thermal evolution stage and hydrocarbon generation contribute little to the pore pressure difference in coal reservoirs of the western Guizhou region.

4) In the western Guizhou region, the present-day *in-situ* stress field, basement structure and tectonic activity may be the dominant factors affecting the lateral pore pressure difference. The sealing capacity of caprocks and the present-day *in-situ* stress field are significant parameters causing vertical pore pressure differences in coal reservoirs.

Acknowledgements We would like to express our gratitude to the reviewers for offering their constructive suggestions and comments which improved this manuscript in many aspects. This work was supported by Natural Science Foundation of Jiangsu Province, China (No. BK20201349), National Natural Science Foundation of China (Grant Nos. 41702130 and 41971335), and Priority Academic Program Development of Jiangsu Higher Education Institutions (PAPD).

References

Chen S D, Tang D Z, Tao S, Xu H, Li S, Zhao J L, Ren P F, Fu H J (2017). *In-situ* stress measurements and stress distribution characteristics of coal reservoirs in major coalfields in China: implication for coalbed methane (CBM) development. Int J Coal Geol, 182: 66–84

Dasgupta S, Chatterjee R, Mohanty S P (2016). Magnitude, mechanisms, and prediction of abnormal pore pressure using well data in the Krishna-Godavari Basin, east coast of India. AAPG Bull, 100(12): 1833–1855

Dou X Z (2012). Tectonic evolution and its control on coalbed methane reservoiring in western Guizhou. Dissertation for the Doctoral Degree. Xuzhou: China University of Mining and Technology (in Chinese)

Engelder T, Fischer M P (1994). Influence of poroelastic behavior on the magnitude of minimum horizontal stress, Sh in overpressured parts of sedimentary basins. Geology, 22(10): 949–952

Fu H J, Yan D T, Yang S G, Wang X M, Zhang Z, Sun M D (2020). Characteristics of in situ stress and its influence on coalbed methane development: a case study in the eastern part of the southern Junggar Basin, NW China. Energy Sci Eng, 8(2): 515–529

Haimson B C, Cornet F H (2003). ISRM suggested methods for rock stress estimation. Part 3: hydraulic fracturing (HF) and/or hydraulic testing of pre-existing fractures (HTPF). Int J Rock Mech Min Sci, 40 (7-8): 1011–1020

Hantschel T, Kauerauf A I (2009). Fundamentals of Basin and Petroleum Systems Modeling. Heidelberg: Springer-Verlag

Hunt J M (1990). Generation and migration of petroleum from abnormally pressured fluid compartments. AAPG Bull, 74(1): 1–12

Ju W, Jiang B, Miao Q, Wang J L, Qu Z H, Li M (2018a). Variation of in situ stress regime in coal reservoirs, eastern Yunnan region, south China: implications for coalbed methane production. AAPG Bull, 102(11): 2283–2303

Ju W, Jiang B, Qin Y, Wu C F, Wang G, Qu Z H, Li M (2019). The present-day *in-situ* stress field within coalbed methane reservoirs, Yuwang Block, Laochang Basin, south China. Mar Pet Geol, 102: 61–73

Ju W, Shen J, Qin Y, Meng S Z, Wu C F, Shen Y L, Yang Z B, Li G Z, Li C (2017). *In-situ* stress state in the Linxing region, eastern Ordos Basin, China: implications for unconventional gas exploration and production. Mar Pet Geol, 86: 66–78

Ju W, Shen J, Qin Y, Meng S Z, Li C, Li G Z, Yang G (2018b). *In-situ* stress distribution and coalbed methane reservoir permeability in the Linxing area, eastern Ordos Basin, China. Front Earth Sci, 12(3): 545–554

Ju W, Yang Z B, Qin Y, Yi T S, Zhang Z G (2018c). Characteristics of *in-situ* stress state and prediction of the permeability in the Upper Permian coalbed methane reservoir, western Guizhou region, SW China. J Petrol Sci Eng, 165: 199–211

Khoshnaw F, Jaf P, Farkha S (2014). Pore, abnormal formation and fracture pressure prediction. WIT Trans Ecol Environ, 186: 579–593

Law B E, Spencer C W (1998). Abnormal pressure in hydrocarbon environments. AAPG Mem, 70: 1–11

Li S, Tang D Z, Pan Z J, Xu H, Guo L L (2015). Evaluation of coalbed methane potential of different reservoirs in western Guizhou and eastern Yunnan, China. Fuel, 139: 257–267

Liu R, Liu J Z, Zhu W L, Hao F, Xie Y H, Wang Z F, Wang L F (2016). *In-situ* stress analysis in the Yinggehai Basin, northwestern South China Sea: implication for the pore pressure-stress coupling process. Mar Pet Geol, 77: 341–352

Neuzil C E (1993). Low fluid pressure within the Pierre Shale: a transient response to erosion. Water Resour Res, 29(7): 2007–2020

Osborne M J, Swarbrick R E (1997). Mechanisms for generating overpressure in sedimentary basins: a reevaluation. AAPG Bull, 81 (6): 1023–1041

Qin Y, Moore T A, Shen J, Yang Z B, Shen Y L, Wang G (2018). Resources and geology of coalbed methane in China: a review. Int Geol Rev, 60(5-6): 777–812

Qin Y, Xiong M H, Yi T S, Yang Z B, Wu C F (2008). On unattached multiple superposed coalbed methane system: in a case of the Shuigonghe syncline, Zhijin-Nayong Coalfield, Guizhou. Geol Rew, 54(1): 65–70 (in Chinese)

Qiu Y X, Zhang Y C, Ma W P (1999). Tectonic Attribute and Evolution of Mountain Xuefeng: A Formation Model for Intracontinental Orogenic Belt. Beijing: Geological Publishing House (in Chinese)

Saxena V, Krief M, Adam L (2018). Handbook of Borehole Acoustics and Rock Physics for Reservoir Characterization. Amsterdam: Elsevier

Shen Y L, Qin Y, Wang G, Xiao Q, Shen J, Jin J, Zhang T, Zong Y, Liu J B, Zhang Y J, Zheng J (2019). Sealing capacity of siderite-bearing strata: the effect of pore dimenstion on abundance and micromorphology type of siderite in the Lopingian (Late Permian) coal-bearing strata, western Guizhou province. J Petrol Sci Eng, 178: 180–192

Singha D K, Chatterjee R (2014). Detection of overpressure zones and a statistical model for pore pressure estimation from well logs in the Krishna-Godavari Basin, India. Geochem Geophys Geosyst, 15(4): 1009–1020

Tang S L, Tang D Z, Xu H, Tao S, Li S, Geng Y G (2016). Geological mechanisms of the accumulation of coalbed methane induced by

hydrothermal fluids in the western Guizhou and eastern Yunnan regions. J Nat Gas Sci Eng, 33: 644–656

Thakur P, Schatzel S, Aminian K (2014). Coal Bed Methane: From Prospect to Pipeline. Amsterdam: Elsevier

Tingay M R P, Hillis R R, Morley C K, Swarbrick R E, Okpere E C (2003). Pore/pressure coupling in Brunei Darussalam-implications for shale injection. In: van Rensbergen P, Hillis R R, Maltman A J, Morley C K, eds. Subsurface Sediment Mobilization. Geological Society, London: Special Publications, 216: 369–379

Tingay M R P, Hillis R R, Swarbrick R E, Morley C K, Damit A R (2009). Origin of overpressure and pore-pressure prediction in the Baram province, Brunei. AAPG Bull, 93(1): 51–74

Veeken P C H (2007). Seismic Stratigraphy, Basin Analysis and Reservoir Characterisation. Amsterdam: Elsevier

Wu C F, Wang C, Jiang W (2014). Abnormal high-pressure formation mechanism in coal reservoir of Bide-Santang Basin, western Guizhou Province. Earth Sci, 39(1): 73–77 (in Chinese)

Wu Y P (2005). The formation mechanisms of abnormal pressure and factor in control of the coal bed gas in Qinshui Basin. Dissertation for the Master's Degree. Chengdu: Chengdu University of Technology (in Chinese)

Xie X, Bethke C M, Li S, Liu X, Zheng H (2001). Overpressure and petroleum generation and accumulation in the Dongying Depression of the Bohaiwan Basin, China. Geofluids, 1(4): 257–271

Xu B B, He D M (2003). Coal Geology in Guizhou Province. Xuzhou: China University of Mining and Technology Press (in Chinese)

Xu H, Tang D Z, Qin Y, Meng C Z, Tao S, Chen Z L (2011). Characteristics and origin of coal reservoir pressure in the west Guizhou area. J China Univ Min Technol, 40(4): 556–560 (in Chinese)

Xu H, Zhang J F, Tang D Z, Li M, Zhang W Z, Lin W J (2012). Controlling factors of underpressure reservoirs in the Sulige gas field, Ordos Basin. Pet Explor Dev, 39(1): 70–74

Yao S, Wu C F, Yang C Q, Li R Q, Chen Y L (2019). Study on pressure characteristics and difference causes of coal reservoirs in Bide-Santang Basin of western Guizhou. Coal Sci Technol, 47(4): 162–168 (in Chinese)

Ye J P, Qin Y, Lin D Y (1998). Coalbed Methane Resources of China. Xuzhou: China University of Mining and Technology Press (in Chinese)

Zahid K M, Uddin A (2005). Influence of overpressure on formation velocity evaluation of Neogene strata from the eastern Bengal Basin, Bangladesh. J Asian Earth Sci, 25(3): 419–429

Zhang J C (2011). Pore pressure prediction from well logs: methods, modifications, and new approaches. Earth Sci Rev, 108(1-2): 50–63